Eco-Biology of Photosynthetic Picoeukaryotes in a Monsoon Influenced Tropical Bay: A Flow Cytometric and Chemotaxonomic Approach

Smita Mitbavkar (mitbavkars@nio.org)
National Institute of Oceanography
Samantha D'souza
National Institute of Oceanography

Research Article

Keywords: Picoeukaryote community, Chemotaxonomy, Pigment biomass, Flow cytometry, Tropical bay, Picodiatoms

Posted Date: September 3rd, 2021

DOI: https://doi.org/10.21203/rs.3.rs-860143/v1

Abstract

The composition and ecology of photosynthetic picoeukaryotes (PPEUK) are essential for microbial food web functioning. We hypothesize that the simultaneous use of flow cytometry (FCM) and High-Performance-Liquid-Chromatography (HPLC) tools will aid in discerning the dominant PPEUK groups contributing to abundance and biomass under prevailing environmental conditions. The PPEUK seasonal community abundance and pigment biomass were investigated from a south-west monsoon influenced tropical bay from June 2015-May 2016. A size-fractionated (< 3 µm) approach using FCM and HPLC revealed five and six PPEUK groups, respectively. Picocryptophytes dominated the PPEUK biomass under varied environmental conditions, whereas Picodiatoms contributed substantially, being abundant under turbulent, low-temperature, nutrient ($NO3^-$, $SiO44^-$) enriched conditions. The Picochlorophytes dominated the community numerically. The relatively higher abundance and biomass of Picoprasinophytes and a positive correlation with $NO3^-$ and $NH4^+$ imply proliferation under higher nutrient concentrations. The least contributors to biomass were Picodinoflagellates and Picoprymnesiophytes. The relatively larger cell size of Picocryptophytes and Picodiatoms resulted in higher cumulative biomass, signifying their role in the microbial food web. Our study proposes incorporation of additional indicator pigments in algorithms used to estimate coastal picophytoplankton contribution to total phytoplankton biomass to avoid discrepancies.

Introduction

Picophytoplankton (Pico; < 3 µm) are known to contribute significantly to the phytoplankton biomass not only in the oligotrophic regions [1] but also in the coastal and estuarine waters [2, 3]. *Synechococcus* (*SYN*) and photosynthetic picoeukaryotes (PPEUK) are the two major groups representing the Pico community in the coastal ecosystems. The Pico form the base of the microbial food web and are linked to the classical food web through the heterotrophic nanoflagellates [4]. The PPEUK are single-celled and diverse [5], representing the smallest size class of protists (0.2–2 µm) [3], which are important contributors of marine plankton biomass and primary production in coastal and oceanic environments [6].

The PPEUK community composition can be estimated through molecular approaches [5]. However, picoplanktonic protists' diversity surveys show that the former method gives a significantly biased view of diversity with a dominance of heterotrophic groups over photosynthetic/mixotrophic groups, as revealed through epifluorescence microscopy [7]. The whole-cell Fluorescence In Situ Hybridization (FISH) method allows the detection and enumeration of particular taxa targeted by specific oligonucleotide probes. However, the relevance of FISH on natural communities depends mainly on the set of probes available [8]. The phytoplankton size-fractionated pigment analysis using High Performance Liquid Chromatography (HPLC) can provide detailed information on the pigment composition, from which the algal classes along with their contribution to the total chlorophyll-*a* (chl-*a*) biomass can be estimated. In addition to biomass, the information on group specific cell abundance is also vital for understanding the biological responses to environmental conditions, which will influence the energy supply and food quality

that fuels production in food webs [9]. Flow cytometry (FCM) is an efficient tool for assessing the Pico community abundance wherein the groups are differentiated based on the cell size and pigment fluorescence intensity [10, 11].

Although many studies have reported the presence of PPEUK from coastal regions, not much information is available on its community dynamics, in terms of numbers and chl-*a* biomass, on a seasonal scale from tropical ecosystems [12]. Given this, we carried out an investigation in a tropical bay influenced by the south-west monsoon to assess the PPEUK diversity and ecology based on the size-fractionated (< 3 µm) pigment composition and cell abundance. The Dona Paula Bay, situated at the confluence of the Zuari estuary's mouth and the Arabian Sea, is influenced by the seasonal hydrography controlled by the riverine freshwater influx and tides [13]. The chl-*a* biomass and species composition of net phytoplankton, especially diatoms, in the bay are well documented [14], with marked monsoonal blooms (June to September) and high biomass during the post-monsoon (October to January). The information on the Pico has been steadily increasing, highlighting their significant role in this ecosystem [15] with a contribution of ~ 20 to 40% to the total chl-*a* biomass annually [14]. The size-fractionated biomass estimations have shown the relevance of > 3 µm phytoplankton biomass and significant contribution by the Pico (< 3 µm) in the estuarine waters of this region [15]. Among the Pico groups, the cyanobacteria, *Synechococcus* (*SYN*) were the significant contributors to the Pico abundance and carbon biomass, with a substantial contribution from the PPEUK [3]. However, information on PPEUK composition is not available from the Indian estuarine waters on a seasonal scale. Such data can aid studies related to ecology and food web dynamics [16]. The aim of this investigation was to (i) determine the seasonal PPEUK composition and abundance through size-fractionated analysis of the < 3 µm fraction *via* HPLC and FCM approach, (ii) estimate the relative contribution of PPEUK and Picocyanobacteria to the total chl-*a* biomass, and (iii) assess the correlation of the biological parameters with the prevalent environmental conditions through the monsoon and the non-monsoon seasons to unravel the PPEUK community dynamics in monsoon-influenced tropical regions. We hypothesize that the simultaneous use of FCM and HPLC tools will aid in discerning the dominant PPEUK groups contributing to abundance and biomass under prevailing environmental conditions.

Materials And Methods

Study Area and Sampling

The study area of Dona Paula Bay (Fig. 1), located in the state of Goa along the west coast of India, experiences a seasonal influence of monsoonal precipitation, freshwater runoff from the Zuari River, and tidal effect [13]. The sampling was carried out bi-monthly between 11:00 h and 12:00 h from June 2015 to May 2016, encompassing three seasons, i.e., the monsoon (MON; June to September), the post-monsoon (PoM; October to January) and the pre-monsoon (PrM; February to May). We collected water samples (~1m below surface) from a jetty at a fixed location (15^{o}27.5' N; 73^{o} 48' E) for monitoring the environmental (water temperature, transparency, salinity, nutrients [nitrate (NO_3^-), nitrite (NO_2^-),

ammonium (NH_4^+), phosphate (PO_4^{3-}), and silicate (SiO_4^{4-})]) and biological (total chl-*a*, Pico pigments and cell abundance) parameters.

Sample Analyses

The measurements of water parameters were carried out by following standard protocols [18]. The water temperature and transparency were measured in the field with a thermometer and a Secchi disc (SD), respectively. The salinity was measured with an autosal in the laboratory. The nutrient concentrations were measured using a nutrient analyzer (Skalar technologies). The water samples collected for the total chl-*a* analysis (1 L) were filtered through GF/F (0.7 µm) filters in the laboratory. The samples for pigment analysis (1 L) were vacuum filtered through 3 µm nucleopore polycarbonate membrane filters. An aliquot of the filtrate (1.8 mL) was preserved in paraformaldehyde (0.2% final concentration) and stored at -80^oC for flow cytometric analysis of picophytoplankton abundance and composition. The remaining filtrate was subsequently filtered on to GF/F filters (0.7 µm) for pigment analysis. The filters were stored at -80^oC until analyses.

The pigments were extracted from the filters in 3 mL of 90% acetone, sonicated with an ultrasonic probe (Labsonic U, B. Braun Biotech International, Leverkusen, Germany) for 10s at 20 kHz and then incubated at -20^oC overnight. The extracts were filtered through 0.2 µm pore size (Nylon filter membranes) syringe filters to remove the debris. The filtered section was added to a 5 mL amber-colored glass vial and placed into a temperature-controlled tray for pigment analyses [19].

The analyses were carried out on an HPLC system (Agilent 1200 series, Agilent Technologies, USA) equipped with a quaternary pump, an auto-sampler, a column temperature controller, a diode-array detector for the separation of the pigments, and an Agilent C8 reverse-phase analytical column maintained at 60^oC (150 x 4.6 mm, 3.5 µm particle size) with 3 phase linear solvent program at a flow rate of 1.1 mL/min. Before injecting into the autosampler, a 0.5 M ammonium acetate (70:30 volume ratio) was added to each sample and standard. A sub-sample of the extract was injected into the auto-sampler. The absorption of the extracted pigments was detected at 450 and 665 nm.

The system was calibrated with commercially available pigment standards (DHI Inc, Denmark; Sigma-Aldrich, USA). The individual pigment peaks were identified by comparing the retention times of the standards with those of the extracts of cultures of selected phytoplankton species belonging to the main algal classes. The individual pigments from the sample extracts were identified by the shape of the peak and their retention time. The concentration of each pigment was calculated from the area of its peak. The pigments obtained from the sample analyses included chlorophylls (*a*, *b*), fucoxanthin, peridinin, 19'-hexanoyloxyfucoxanthin (19'HF), 19'-butanoyloxyfucoxanthin (19'BF), alloxanthin, neoxanthin, prasinoxanthin, violaxanthin, lutein, and zeaxanthin.

The Chemical Taxonomy program (CHEMTAX version 1.95) [20] was used to calculate the algal class composition and the contribution of the different algal classes to the Chl-*a*. The pigment groups were

defined on the basis of pigment composition and pigment ratios normalized to chl-*a* (Table 1). The initial signature pigments:chl-*a* ratios were obtained from [21]. Seven algal groups were determined in the Pico fraction, i.e., Picocyanobacteria, Picocryptophytes, Picodiatoms, Picochlorophytes, Picoprasinophytes, Picodinoflagellates, and Picoprymnesiophytes. These algal groups have representatives in the nano- and microphytoplankton (> 3 µm) in the marine environment.

The Pico samples were analysed with the BD FACS Aria-II FCM with laser excitation wavelengths of 488 nm (blue laser) and 630 nm (red laser). Single cells were characterized based on their optical characteristics: forward-angle light scatter (FALS; proxy for cell size), right-angle light scatter (RALS), and red (chlorophyll and phycocyanin pigments) and orange (phycoerythrin pigment) fluorescence [11, 22]. Fluorescent beads of 2 µm ('Fluoresbrite', Polysciences) diameter were used as internal standards to normalize the fluorescence and size parameters. The BD FACS Diva software was used for the data analysis. The FCM signatures were plotted into several two-dimensional cytograms that facilitated the manual identification of different groups.

FCM analyses revealed seven clusters based on the optical properties. Two groups were attributed to Picocyanobacteria, i.e., *SYN* with small size and orange and red fluorescence peaks due to phycoerythrin and phycocyanin pigments, respectively (both combined hereafter). Five groups were assigned to PPEUK i.e., Picocryptophytes based on the relatively high amounts of phycoerythrin and large cell size compared to *SYN*, Picodiatoms based on the relatively high chl fluorescence and cell size as this group comprises large and chl rich cells, Picochlorophytes-I and II based on the chl fluorescence and cell size lower than that of the Picodiatoms, and Picoprasinophytes based on the smaller size and lower chl fluorescence intensity than the Picochlorophytes Picodinoflagellates and Picoprymnesiophytes could not be determined in the FCM dot plot due to their lower numbers (Fig. 5).

Data Analyses

A redundancy analysis (RDA) was conducted to explore the multivariate relationship between abundance and chl-*a* biomass of the Pico groups [log (x+1) transformed] and the recorded environmental variables. The linear response model was selected based on the lengths of the environmental gradient tested (< 2 standard deviations) through the detrended correspondence analysis (DCA). Six environmental variables were used as independent variables: rainfall, temperature, SD depth, salinity, nutrients, and Chl-*a* concentration. The direct gradient technique of RDA was performed using forward selection (and a Monte-Carlo permutation test, n = 499) to determine a subset of significant environmental variables explaining the individual variation of the Pico groups. The RDA was conducted using the CANOCO v4.5 software [23].

Results

Environmental Parameters

The highest rainfall was observed during the first half of June, the second half of July, and early September. The water temperature exhibited a bimodal pattern with peaks during the late PrM and early PoM, and the annual variation ranged between 23ºC and 34ºC. Salinity distribution followed a trend opposite to rainfall with the lowest values during MON (25 ± 6) and highest during the PrM (34.5 ± 1.3) and PoM (33 ± 2.5). The SD depth was relatively higher during the PoM (170 ± 43 m) and PrM (106 ± 56 m) than during the MON season (73 ± 30 m) (Fig. 2a-d). The NO_3^- + NO_2^-, PO_4^{3-}, and SiO_4^{4-} concentrations were higher during MON. The NH_4^+ concentrations were higher during MON and PrM (Table 2).

Seasonal variability in the chlorophyll-*a* concentrations

The total chl-*a* concentration during the MON season ranged between 1327 ng L^{-1} (July 29) and 5960 ng L^{-1} (August 6) (Fig. 3). During the PoM season, the chl-*a* concentrations ranged between 1195 ng L^{-1} (Nov 4) and 7246 ng L^{-1} (Nov 6). During PrM, the chl-*a* concentrations ranged between 828 ng L^{-1} (April 22) and 3308 ng L^{-1} (May 09). The seasonal trend was MON (3570 ± 1600 ng L^{-1}) > PoM (3150 ± 1750 ng L^{-1}) > PrM (1740 ± 830 ng L^{-1}).

The concentration of chl-*a* in the < 3 µm fraction ranged from 216 ng L^{-1} (Sept 28) to 2775 (August 6th) ng L^{-1} during MON, 84 ng L^{-1} (Jan 30) to 1289 ng L^{-1} (October 15) during PoM, and 41 ng L^{-1} (May 25) to 577 ng L^{-1} (April 22nd ‘016) during PrM (Fig. 3). The seasonal trend was MON (860 ± 660 ng L^{-1}) > PoM (400 ± 370 ng L^{-1}) > PrM (290 ± 190 ng L^{-1}).

The seasonal contribution of < 3 µm fraction to the total chl-*a* biomass was higher during MON (25.8 ± 13.8%) followed by PrM (22.1 ± 21.4%) and PoM (12.1 ± 6.7%) (Fig. 3). A significant positive correlation was observed between the total chl-*a* and < 3 µm *a* biomass (R^2 = 0.7; P < 0.01).

Seasonal Variability in the Picophytoplankton Biomass

The CHEMTAX analysis of the < 3 µm fraction chl-*a* data revealed the contribution from 7 algal groups to the Pico chl-*a* biomass, comprising one group of Picocyanobacteria and six groups of PPEUK (Table 1). During the MON, a significant portion of the Pico chl-*a* biomass was contributed by the PPEUK (468 ng L^{-1}; 58.3%) and the rest by Picocyanobacteria (388 ng L^{-1}; 41.7%). During PoM, the PPEUK contributed 61.7% (234 ng L^{-1}) and Picocyanobacteria 38% (166 ng L^{-1}). During PrM, the PPEUK and Picocyanobacteria contributed 57.4% (173 ng L^{-1}) and 42.6% (121 ng L^{-1}), respectively (Fig. 4).

The PPEUK exhibited a variable community structure with respect to the seasons. The hydrography and environmental conditions during the MON season were driven by the precipitation intensity and freshwater runoff. At the initiation of the sampling period, under high saline (35) conditions, the Picoprasinophytes (33.8%) and Picochlorophytes (31.6%) were the dominant contributors to the PPEUK chl-*a* biomass. The dominance later shifted to the Picocryptophytes (42.8%) and Picodiatoms (50.5%), following a decline in salinity (20 to 25 and < 20, respectively). The subsequent rise in salinity, following a break-in precipitation (30), coincided with an increase in the Picoprasinophytes (36.7%) followed by the

Picocryptophytes (43%; salinity 25) contribution. Towards the end of the MON season (salinity 30), the Picocryptophytes (52%) and Picodiatoms (43.4%) dominated the PPEUK community while the Picocryptophytes dominated during the PoM (37.2%) and PrM (54.7%) seasons (Fig. 4).

Seasonal Variability in the Picophytoplankton Abundance

Seasonally, during the MON, a major portion of the Pico abundance was contributed by *SYN* (35.6×10^3 cells mL^{-1}; 74.3%) and rest by PPEUK (13.2×10^3 cells mL^{-1}; 25.7%). During PoM, the *SYN* contributed 80.6% (44.6×10^3 cells mL^{-1}) and PPEUK 19% (8.3×10^3 cells mL^{-1}). During the PrM, *SYN* contributed 87.9% (95.6×10^3 cells mL^{-1}) and PPEUK 12.1% (14.6×10^3 cells mL^{-1}), respectively (Fig. 6a). Throughout the sampling, the cell abundance of the *SYN* (1.95×10^3 to 210×10^3 cells mL^{-1}) and PPEUK (0.18×10^3 to 54.5×10^3 cells mL^{-1}) exhibited a similar seasonal distribution pattern with a significant positive correlation ($R^2 = 0.74$; $P < 0.001$). The seasonal trend for the *SYN* abundance was PrM ($95 \pm 78 \times 10^3$ cells mL^{-1}) > PoM ($45 \pm 39 \times 10^3$ cells mL^{-1}) > MON ($36 \pm 31 \times 10^3$ cells mL^{-1}). The PPEUK abundance exhibited the following seasonal average trend; PrM ($14.6 \pm 17.5 \times 10^3$ cells mL^{-1}) > MON ($13 \pm 13 \times 10^3$ cells mL^{-1}) > PoM ($8.3 \pm 5.4 \times 10^3$ cells mL^{-1}).

At the beginning of the sampling (MON season), before the decline in salinity due to precipitation and freshwater runoff into the Bay (salinity: 35), the Picochlorophytes-II were the dominant contributors (76%) to the PPEUK abundance. Subsequently, the decline of salinity (20 to 25) and temperature led to a change in the community dominance to Picoprasinophytes (50%). The further decline in salinity (< 20) resulted in the Picochlorophytes-I (52.3%) dominating the community with an increased contribution from the Picocryptophytes (18.4%). The dominance continued with the following rise in salinity (~30), but the contribution from Picochlorophytes-II (27.5%) and Picocryptophytes (24.8%) increased. A salinity of 25 led to an increased contribution from the Picoprasinophytes (22%) with dominance by Picochlorophytes-II (40.8%) that continued till the end of the MON season (69%) with an increase in salinity (30). The Picodiatoms increase (7%) during this period. During the PoM, the Picochlorophytes-I dominated the community (49.3%) with intermittent dominance of the Picochlorophytes-II (24.6%) and Picoprasinophytes (16%). During the PrM, the community was dominated by the Picochlorophytes-I (57%) (Fig. 6b-f).

Relationship of the Pico with the Environmental Parameters

During MON, the first 2 RDA axes explained 79.2% of the variability in the Pico groups' biomass and 94.2% of the relationship between biomass and the environmental variables (Fig. 7a). The temperature and NO_3^-+NO_2^- were the significant explanatory variables (Table 3). The Picocryptophytes positively correlated with nutrients (NH_4^+, NO_3^-+NO_2^-) and total chl-*a* and negatively with salinity, temperature, and SD depth. The Picodiatoms correlated positively with nutrients (NO_3^-+NO_2^-, SiO_4^{4-}), rainfall, total chl-*a,* and negatively with salinity, temperature, and SD depth. The Picochlorophytes positively correlated with nutrients (NH_4^+, NO_3^-+NO_2^-) and negatively with salinity, temperature, and SD depth. The

Picoprasinophytes were positively correlated with temperature, salinity, NO_3^-+NO_2^-, and SD depth. The Picocyanobacteria positively correlated with salinity, temperature, and SD depth. In the abundance triplot (Fig. 7b), the first 2 RDA axes explained 46.1% of the variability in the Pico groups' abundance and 96.2% of the relationship between abundance and the environmental variables (Fig. 7b; Table 4). The Picocryptophytes were positively correlated with nutrients (PO_4^{3-}, NH_4^+) and negatively with salinity, temperature, and SD depth. The Picodiatoms correlated positively with salinity, temperature, SD depth, and SiO_4^{4-}. The Picochlorophytes were positively correlated with salinity, temperature, and SD depth. The Picoprasinophytes were positively correlated with SD depth, PO_4^{3-} and NH_4^+. The Picocyanobacteria positively correlated with temperature, SD depth, NH_4^+, and PO_4^{3-}.

During PoM, the first 2 RDA axes explained 88.8% of the variability in the Pico groups' biomass and 91.7% of the relationship between biomass and the environmental variables (Fig. 7c). The Picocryptophytes were positively correlated with nutrients (NH_4^+, NO_3^-+NO_2^-). The Picodiatoms correlated positively with temperature, SiO_4^{4-} and total chl-*a* and negatively with NO_3^-+NO_2^-. The Picoprasinophytes were positively correlated with NH_4^+ and PO_4^{3-}. The Picochlorophytes did not exhibit any significant relationship. The Picocyanobacteria positively correlated with temperature and total chl-*a*. In the abundance triplot (Fig. 7d), the first 2 RDA axes explained 74.6% of the variability in the abundance of the Pico groups and 92.2% of the relationship between abundance and the environmental variables (Fig. 7d). The Picodiatoms positively correlated with the SD depth. The PPEUK groups and *SYN* did not show any significant correlation with the nutrients.

During PrM, the first 2 RDA axes explained 95.5% of the variability in the biomass of the Pico groups and 95.5% of the relationship between biomass and the environmental variables (Fig. 7e). The Picodiatoms positively correlated with PO_4^{3-}. The Picocryptophytes, Picochlorophytes, and Picoprasinophytes positively correlated with NH_4^+, NO_3^-+NO_2^- and the SD depth. The Picoprymnesiophytes and picodinoflagellates correlated positively with NO_3^-+NO_2^-. The Picocyanobacteria were positively correlated with NO_3^-+NO_2^-. In the abundance triplot, the first 2 RDA axes explained 98.5% of the variability in the Pico groups' abundance and 98.5% of the relationship between abundance and the environmental variables (Fig. 7f). All the PPEUK groups correlated positively with PO_4^{3-} and NO_3^-+NO_2^- except the Picoprasinophytes, which correlated with only PO_4^{3-}. Also, the Picodiatoms positively correlated with SiO_4^{4-}. The Picocyanobacteria positively correlated with PO_4^{3-}.

Discussion

Picoeukaryotic Abundance and Biomass: A Global Comparison

The size-fractionated approach with the FCM and HPLC-CHEMTAX calculations yielded vital information about the PPEUK in terms of abundance and biomass. The Pico community was dominated by the Picocyanobacteria in terms of numbers and PPEUK in terms of chl-*a* biomass. The PPEUK group contribution to the Pico biomass in the present study (> 50%) was similar to that reported for the Chesapeake Bay sub-estuary (45%) [24] and the coastal Baltic Sea (~ 50%) [25]. The dominance of the PPEUK community by the Picocryptophytes and the Picochlorophytes, in terms of chl-*a* biomass and cell abundance, respectively was similar to that reported in other regions [24, 25, 8].

The relatively larger cell size of the Picocryptophytes resulted in a higher cumulative contribution (40.3%) to the PPEUK biomass, in spite of their low numerical representation (7%). Such observations have been reported from coastal regions [26]. The ecological importance of these photosynthetic flagellates has been established not only in the nanoplanktonic [27] but also the PPEUK communities in coastal waters through molecular methods with a relatively higher contribution to the picoplankton composition than to the total eukaryotic plankton diversity [28]. This group possesses high contents of EPA and DHA [29], which could serve as food of high nutritional quality for the consumers. The Picocryptophytes belonging to genus *Hillea* are known to represent some coastal PPEUK communities [30], but there is still uncertainty about cells passing through the filter paper during size-fractionation. Our study verified this by examining the same samples with and without filtration *via* FCM, which showed the presence of cryptophytes in the unfiltered and < 3 µm fractions.

Although the numerical representation of the Picodiatoms was low (4%), their larger cell size contributed substantially to the PPEUK biomass (25.9%). [31] reported almost 20 diatom species representing the PPEUK community. In our study, the highest contribution of the Picodiatoms to the PPEUK biomass on July 21st 2015 (70%) coincided with a *S. costatum* bloom in the water column (personal observation) with a cell width of 2–4 µm. Earlier studies have reported small-sized (< 3 µm) *Skeletonema* species [32, 33]. However, the marker pigment of diatoms (fucoxanthin) is also present in other phytoplankton classes such as the chrysophyceae, pelagophyceae, and prymnesiophyceae, all of which have members in the < 3 µm size fraction. There could be some contribution from the bolidophyceae class [34] that includes small heterokont flagellates e.g. *Bolidomonas pacifica, Bolidomonas* mediterranea, whose diagnostic pigment fucoxanthin and 18S rRNA gene sequences are similar to those of diatoms [35]. The fucoxanthin could also be from small-sized (1–2 µm in width) diatoms, and ~ 70% of this pigment was observed in the < 1 µm fraction in the Urdabai estuary, Spain [36]. Molecular studies have also reported sequences of diatoms in the Mediterranean Sea [37] and the Canadian Arctic Basin [12] in the Pico fraction. Although these sequences could have come from undescribed small diatoms, there is a possibility of diatoms or male gametes of larger diatoms passing through filter pores [38]. A bloom of the picodiatom species, *Minutocellus polymorphus* (1 x 10^5 cells mL^{-1}) was observed in the Mediterranean lagoon [32].

The Picochlorophytes dominated the PPEUK community in terms of numbers (71.6%) but not biomass (17%) throughout the study period. Our results are close to that reported for the English Channel using FISH-TSA, wherein an average of 85% of PPEUK were assigned to chlorophytes [39]. The Picoprasinophytes that dominate the marine PPEUK community are relatively abundant in coastal waters

than the oceanic regimes [41]. The marine Picoprasinophyte algae *Bathycoccus, Ostreococcus*, and *Micromonas* belonging to the class Mamiellophyceae are widespread [5], amongst which, *Micromonas* numerically dominates the coastal PPEUK community biomass [40]. These species are among the smallest unicellular eukaryotes known.

The dinoflagellates contributed a small percentage of the PPEUK biomass (1.5%). Due to their lower numbers, distinguishing them in the FCM was tedious. Earlier studies reported this group in the < 3 μm biomass of coastal waters [24, 25, 42]. Several sequences from this class were recovered and attributed to either some unidentified PPEUK species or life cycle stages of existing dinoflagellate species [37]. However, previous studies have doubted the presence of dinoflagellates in this fraction and considered it to a methodical artefact wherein cells must have crept through the filter paper during filtration [5], or else they may be broken parts of cells [16]. This aspect needs further clarification with detailed studies.

The Picoprymnesiophytes, the least contributor to the PPEUK biomass (0.6%) were observed on rare occasions throughout the study period with higher representation during the non-MON seasons. They are most important in the open ocean [43], with few representatives in the coastal and freshwater ecosystems [44]. Due to their lower numbers, distinguishing them in the FCM was tedious. Their higher representation in the coastal waters [45] during the non-monsoon could indicate advection from the offshore waters due to increased tidal influence in the Dona Paula Bay, as corroborated by the positive correlation with salinity. Usually, this group in the larger size fraction is reported during the non-bloom conditions [46] and is known to dominate the oligotrophic waters [35].

Environmental influence on the seasonal abundance and biomass of the picoplankton community

The Picocyanobacteria preferred higher salinity, temperature, and water transparency as reflected in its higher abundance during the MON precipitation breaks when the NO_3^- concentrations were also increased. This group is also known to prefer high NH_4^+ [47] and PO_4^{3-} concentrations along with high temperatures [48], as observed during the warmer PrM.

The cryptophytes possess multiple traits that make them successful in varied environmental conditions. First and foremost, their presence throughout the study period depicts a euryhaline nature [49]. During the MON, the Picocryptophytes usually dominated the biomass after an episode of salinity drop due to freshwater influx, as seen from the negative correlation with the salinity. Although high nutrient influx from freshwater input enhances phytoplankton growth rates in the Dona Paula Bay, there is a corresponding reduction in light availability in the water column [14]. In our study, the PPEUK biomass dominance by the Picocryptophytes during the MON could be explained by their ability to sustain adverse and light-limited environments as they possess physiological adaptations such as the green light-harvesting phycobiliproteins and photoacclimation [50], as corroborated by the negative and positive correlation with the SD depth and the total chl-*a*, respectively. A higher biomass yield and a lower growth rate under the low light condition for phytoplankton have been shown with N and P additions [51]. In our study, the positive correlation of its abundance with NH_4^+ during the MON shows its preference for the

regenerated nutrients for multiplication. A cryptophyte bloom was reported in the lower reaches of a Mediterranean river estuary of the eastern Adriatic Sea during slower river flow and increased orthophosphate and NH_4^+ concentrations [52]. The positive relation of this group with NO_3^- and PO_4^{3-} during the PrM could suggest its capability to utilize all kinds of inorganic nutrients. They also exhibit mixotrophy and use dissolved organic carbon to enhance their growth requirements [53]. In the Dona Paula Bay, dissolved organic matter is derived from autochthonous production, sediment pore waters and allochthonous sources e.g., adjacent Mandovi and Zuari estuaries [54].

The Picodiatom contribution to the < 3 µm PPEUK biomass was dominant under the turbulent, low temperature, nutrient (NO_3^-, SiO_4^{4-}) enriched conditions during the MON season as corroborated by the RDA. Similar distribution patterns are reported in the larger phytoplankton size fraction [14, 47] since diatom species react rapidly to nutrients or silica addition [55]. The positive correlation with total chl-*a* biomass implies that these conditions promote their contribution. In the present study, the higher concentrations of nutrients during the MON (NO_3^- and SiO_4^{4-}) and early PoM (SiO_4^{4-}) could be responsible for their relatively higher contribution to the chl-*a* biomass [11]. However, the lower biomass and higher numbers during the PrM may be representing smaller sized species. In the coastal and offshore turbulent nutrient-rich environments, minute diatom taxa such as *Minidiscus* (*M. Trioculatus* and *M. comicus* size up to 1.5 to 1.9 µm, respectively), occasionally contribute significantly to spring blooms [56].

The Picochlorophytes contributed relatively higher biomass during the PrM exhibiting a positive correlation with NH_4^+ concentrations. These groups likely outcompete the diatoms during nutrient-limited conditions and warm water temperatures due to their smaller size and larger surface area: volume ratios [11, 48]. Phytoplankton cell size reduction in response to warming was mediated by nutrient limitation [57]. The relatively higher abundance and biomass of the Picoprasinophytes during the MON season and the positive correlation with NO_3^- and NH_4^+ implies proliferation under higher nutrient concentrations. *Micromonas pusilla* is better adapted to take up NH_4^+ than NO_3^- and urea [58].

Conclusions And Implications

The study highlights the significance of employing different techniques (FCM and HPLC) for investigating the responses of the PPEUK community in terms of biomass and numbers to environmental conditions. PPEUK community contributes substantially to the Pico chl-*a* biomass and numbers throughout the year. The Picocryptophytes dominated the PPEUK biomass signifying a vital role in the tropical microbial food web. Functional group differences in the utilization of N were observed wherein picodiatoms were favoured by NO_3^-, while picocyanobacteria, picochlorophytes, picoprasinophytes, and picocryptophytes may be better adapted to use of NH_4^+ [45]. The results substantiate the general notion that oscillations in the relative nutrient concentrations can favour different phytoplankton groups leading to a shift in biodiversity.

Generally, estimation of the Pico contribution from HPLC analysed total chl-*a* is done with the help of algorithms developed with a limited number of diagnostic pigments such as zeaxanthin, total chl-*b*, and 19' HF [17]. These algorithms may best represent the Pico community of oligotrophic open ocean waters where *Synechococcus* and *Prochlorococcus* dominate. However, in coastal waters, it is evident from our results of the < 3 µm phytoplankton fraction that additional diagnostic pigments such as alloxanthin (cryptophytes) and fucoxanthin (diatoms) form an essential component of the Pico biomass fraction, which need to be incorporated in the algorithms to improve the output.

Declarations

Acknowledgments We would like to thank The Director, National Institute of Oceanography (CSIR) and Dr. A.C. Anil for their support. The CSIR project, 'Ocean Finder' funded this work. We thank Mr. Sathish K. for his help during the HPLC sample analyses. We also thank our project team members for their help and suggestions. This is a NIO contribution (no. #).

Author Contribution S.D. collected and analysed the field samples. S.M. and S.D. performed statistical analyses and wrote the manuscript.

Funding The CSIR project, 'Ocean Finder' funded this work.

Ethics Approval This study does not contain any studies with human participants or animals performed by any of the authors.

Conflict of Interest The authors declare no competing interests.

References

1. Brown SL, Landry MR, Barber RT, Campbell L, Garrison DL, Gowing MM (1999) Picophytoplankton dynamics and production in the Arabian Sea during the 1995 Southwest Monsoon. Deep Sea Res II 46:1745–1768
2. Gaulke AK, Wetz MS, Paerl HW (2010) Picophytoplankton: a major contributor to planktonic biomass and primary production in a eutrophic, river-dominated estuary. Estuar Coast Shelf Sci 90:45–54
3. Mitbavkar S, Patil JS, Rajaneesh KM (2015) Picophytoplantkon as tracers of environmental forcing in a tropical monsoonal bay. Mic Ecol DOI. 10.1007/s00248-015-0599-2
4. Reckermann M, Veldhuis MJW (1997) Trophic interactions between picophytoplankton and micro- and mesozooplankton in the western Arabian Sea during the NE monsoon 1993. Aquat Microb Ecol 12:263–273
5. Massana R (2011) Eukaryotic picoplankton in surface oceans. Annual Rev Microbiol 65:91–110
6. Jardillier L, Zubkov MV, Pearman J, Scanlan DJ (2010) Significant CO_2 fixation by small prymnesiophytes in the subtropical and tropical northeast Atlantic Ocean. ISME J 4:1180–1192

7. Not F, del campo J, Balagué V, de vargas C, Massana R (2009) New insights into the diversity of marine picoeukaryotes. *PLoS ONE* 4:E7143
8. Not F, Valentin K, Romari K, Lovejoy C, Massana R, Töbe K, Vaulot D, Medlin LK (2007) Picobiliphytes: A Marine Picoplanktonic Algal Group with Unknown Affinities to Other Eukaryotes. Science 315:253–255
9. Winder M, Carstensen J, Galloway AWE, Jakobsen HH, Cloern JE (2017) The land-sea interface: a source of high-quality phytoplankton to support secondary production. Limnol Oceanogr 62:5258–5271
10. Marie D, Partensky F, Vaulot D, Brussaard C (1999) Enumeration of phytoplankton, bacteria and viruses in marines samples. In: Robinson JP, Darzynkiewicz D, Dean PN, Orfao A and others (eds) Current protocols in cytometry. John Wiley, New York, NY, p 1–15
11. Read DS, Bowes MJ, Newbold LK, Whiteley AS (2014) Weekly flow cytometric analysis of riverine phytoplankton to determine seasonal bloom dynamics. Environ Sci: Processes Impacts 16:594–603
12. Lovejoy C, Massana R, Pedros-Alio C (2006) Diversity and distribution of marine microbial eukaryotes in the Arctic Ocean and adjacent seas. Appl Environ Microbiol 72:3085–3095
13. Shetye SR, Gouveia AD, Singbal SY, Naik CG, Sundar D, Michael GS, Nampoothiri G (1995) Propagation of tides in the Mandovi-Zuari estuarine network. Proceedings of the Indian Academy of Sciences – Earth and planetary Sciences 104:667–682
14. Patil JS, Anil AC (2015) Effect of monsoonal perturbations on the occurrence of phytoplankton blooms in a tropical bay. Mar Ecol Prog Ser 530:77–92
15. Rajaneesh KM, Mitbavkar S, Anil AC (2018) Dynamics of size-fractionated phytoplankton biomass in a monsoonal estuary: Patterns and drivers for seasonal and spatial variability. Estuar Coast Shelf Sci 207:325–337
16. Rodrı´guez F, Pazosb Y, Maneirob J, Zapataa M (2003) Temporal variation in phytoplankton assemblages and pigment composition at a fixed station of the Rı´a of Pontevedra (NW Spain). Estuar Coast Shelf Sci 58:499–515
17. Brewin RJW, Sathyendranath S, Jackson T, Barlow R, Brotas V, Airs R, Lamont T (2015) Influence of light in the mixed-layer on the parameters of a three-component model of phytoplankton size class. Rem Sensing Environment 168:437–450
18. Parsons TR, Maita Y, Lalli CM (1984) A manual of chemical and biological seawater analysis. Pergamon, New York
19. Roy R, Chitari R, Kulkarni V, Krishna MS, Sarma VVSS, Anil AC (2015) CHEMTAX-derived phytoplankton community structure associated with temperature fronts in the northeastern Arabian Sea. J Mar Syst 144:81–91
20. Mackey CD, Mackey DJ, Higgins HW, Wright SW (1996) CHEMTAX – a program for estimating class abundances from chemical markers: application to HPLC measurements of phytoplankton. Mar Ecol Prog Ser 144:265–283

21. Roy R, Anil P, Gauns M, Naqvi SWA (2006) Spatial variation of phytoplankton pigments along the southwest coast of India. Estuar Coast Shelf Sci 69:189–195
22. Bonato S, Christaki U, Lefebvre A, Lizon F, Thyssen M, Artigas LF (2015) High spatial variability of phytoplankton assessed by flow cytometry in a dynamic productive coastal area, in spring: The eastern English Channel. Estuar Coast Shelf Sci 154:214–223
23. ter Braak CJF, Smilauer P (2002) CANOCO Reference manual and CanoDraw for Windows User's guide: Software for Canonical Community Ordination (version 4.5). Microcomputer Power, Ithaca, New York
24. Ray TR, Haas LW, Sieracki ME (1989) Autotrophic picoplankton dynamics in a Chesapeake Bay sub-estuary. Mar Ecol Prog Ser 52:273–285
25. Tamm M, Laas P, Freiberg R, Noges P, Noges T (2018) Parallel assessment of marine autotrophic picoplankton using flow cytometry and chemotaxonomy. Sci Tot Env 625:185–193
26. Casotti R, Brunet C, Arnone B, Ribera D'Alcala M (2000) Mesoscale features of phytoplankton and planktonic bacteria in a coastal area as induced by external water masses. Mar Ecol Prog Ser 195:15–27
27. Cerino F, Zingone A (2006) A survey of cryptomonad diversity and seasonality at a coastal Mediterranean site. Eur J Phycol 41:363–378
28. Metfies K, Gescher C, Frickenhaus S, Niestroy R, Wichels A, Gerdts G et al (2010) Contribution of the class cryptophyceae to phytoplankton structure in the German Bight. J Phycol 46:1152–1160
29. Ravet JL, Brett MT (2013) A test of the role of polyunsaturated fatty acids in phytoplankton food quality for Daphnia using liposome supplementation. Limnol Oceanogr 48:1938–1947
30. Gracia-Escobar MF, Millán-Núñez R, Valenzuela-Espinoza E, González-Silvera A, Santamaría-del-Ángel E (2015) Changes in the composition and abundance of phytoplankton in a coastal lagoon of Baja California, México, during 2011. Open J Mar Sci 5:169–181
31. Giovagnetti V, Cataldo ML, Conversano F, Brunet C (2012) Growth and photophysiological responses of two picoplanktonic *Minutocellus* species, strains RCC967 and RCC703 (Bacillariophyceae. Eur J Phycol 47:408–420
32. Sarno D, Zingone A, Saggiomo V, Carrada GC (1993) Hydrobiol 271:27–40 &l</bvertical-align:super;&gt
33. Zingone A, Percopo I, Sims PA, Sarno D (2005) Diversity in the genus *Skeletonema* (Bacillariophyceae): I. Are examination of the type material of *S. costatum* with the description of *S. grevillea* sp. nov. J Phycol 41:140–150
34. Guillou L, Che´tiennot-Dinet MJ, Medlin LK, Claustre H, Loiseaux-de Goer S, Vaulot D (1999) Bolidomonas: a new genus with two species belonging to a new algal class, the Bolidophyceae (Heterokonta). J Phycol 35:368–381
35. Vaulot D, Eikrem W, Viprey M, Moreau H (2008) The diversity of small eukaryotic phytoplankton (≤ 3 μm) in marine ecosystems. FEMS Microbiol Rev 32:795–820

36. Ansotegui A, Sarobe A, Trigueros JM, Urrutxurtu I, Orive E (2013) Size distribution of algal pigments and phytoplankton assemblages in a coastal-estuarine environment: contribution of small eukaryotic algae. J Plank Res 25:341–355
37. Massana R, Balagué V, Guillou L (2004) Picoeukaryotic diversity in an oligotrophic coastal site studied by molecular and culturing approaches. FEMS Microbiol Ecol 50:231–243
38. Davidovich NA, Bates SS (1998) Sexual reproduction in the pennate diatoms *Pseudo-nitzschia multiseries* and *P. pseudodelicatissima* (Bacillariophyceae). J Phycol 34:126–137
39. Not F, Latasa M, Marie D, Cariou T, Vaulot D, Simon N (2004) A single species *Micromonas pusilla* (Prasinophyceae), dominates the eukaryotic picoplankton in the western channel. Appl Env Microbiol 70:4064–4072
40. Tragin M, Vaulot D (2018) Green microalgae in marine coastal waters: The ocean sampling day (OSD0 dataset). Sci Rep 8:14020
41. Not F, Massana R, Latasa M, Marie D, Colson C, Eikrem W et al (2005) Late summer community composition and abundance of photosynthetic picoeukaryotes in Norwegian and Barents Seas. Limnol Oceanogr 50:1677–1686
42. Cheung MK, Au CH, Chu KH, Kwan HS, Wong CK (2010) Composition and genetic diversity of picoeukaryotes in subtropical coastal waters as revealed by 454 pyrosequencing. ISME J4:1053–1059
43. Liu H, Probert I, Uitz J, Claustre H and others (2009) Extreme diversity in non-calcifying haptophytes explains a major pigment paradox in open oceans. Proc Natl Acad Sci USA 106:12803–12808
44. Simon M, Lopez-Garcia P, Moreira D, Jardillier L (2013) New haptophyte lineages and multiple independent colonizations of freshwater ecosystems. Environ Micobiol Rep 5:322–332
45. Bandyopadhyay D, Biswas H, Sarma VVSS (2017) Impacts of SW monsoon on phytoplankton community structure along the western coastal BOB: an HPLC approach. Estuar coasts 40:1066–1081
46. Latasa M, Scharek R, Vidal M, Vila-Reixach G, Gutierrez-Rodriguez A, Emelianov M, Gasol JM (2010) Preferences of phytoplankton groups for waters of different trophic status in the northwestern Mediterranean Sea. Mar Ecol Prog Ser 407:27–42
47. Glibert PM, Wilkerson FP, Dugdale RC, Raven JA, Dupont CL, Leavitt PR, Parker AE, Burkholder JA, Kana TM (2016) Pluses and minuses of ammonium and nitrate uptake and assimilation by phytoplankton and implications for productivity and community composition, with emphasis on nitrogen-enriched conditions. Limnol Oceanogr 61:165–197
48. Swarbrick VJ, Simpson GL, Glibert PM, Leavitt PR (2019) Differential stimulation and suppression of phytoplankton growth by ammonium enrichment in eutrophic hardwater lakes over 16 years. Limnol Oceanogr 64:S130–S149
49. Laza-Martinez A, Arluzea J, Miguel I, Orive E (2012) Morphological and molecular characterization of *Teleaulax gracilis* sp. nov. and *T. minuta* sp. nov. (Cryptophyceae). Phycol 51:649–661

50. Spear-Bernstein L, Miller KR (1989) Unique location of the phycobiliprotein light-harvesting pigment in the Cryptophyceae. J Phycol 25:412–419
51. Mustaffa NIH, Kallajoki L, Hillebrand H, Wurl O, Striebel M (2020) Sea surface phytoplankton community response to nutrient and light changes. Mar Biol 167:123
52. Šupraha L, Bosak S, Ljubeši´c Z, Mihanovi´c H, Oluji´c G, Mikac I et al (2014) Cryptophyte bloomin Mediterranean estuary: high abundance of Plagioselmis cf. prolonga in the Krka River estuary (Eastern Adriatic Sea). Sci Mar 78:329–338
53. Gervais F (1997) Light-dependent growth, dark survival, and glucose uptake by cryptophytes isolated from a freshwater chemocline. J Phycol 33:18–25
54. Wafar S, Untawale AG, Wafar MVM (1997) Litter fall and energy flux in a mangrove ecosystem. Estuar Coast Shelf Sci 44:111–124
55. Reynolds CS (1997) Vegetation Processes in the Pelagic. *A Model for Ecosystem Theory.* ECI, Oldendorf
56. Leblanc K, Queguiner B, Diaz F, Cornet V, Michel-Rodriguez M, de Madron XD et al (2018) Nanoplanktonic diatoms are globally overlooked but play a role in spring blooms and carbon export. Nat Comm 9:953
57. Peter KH, Sommer U (2013) Phytoplankton cell size reduction in response to warming mediated by nutrient limitation. PLOS one 8:e71528
58. Cochlan WP, Harrison PJ (1991) Kinetics of nitrogen (nitrate, ammonium and urea) uptake by the picoflagellate *Micromonas pusilla* (Prasinophyceae). J Exp Mar Biol Ecol 153:129–141

Tables

Due to technical limitations, table 1 to 3 is only available as a download in the Supplemental Files section.

Figures

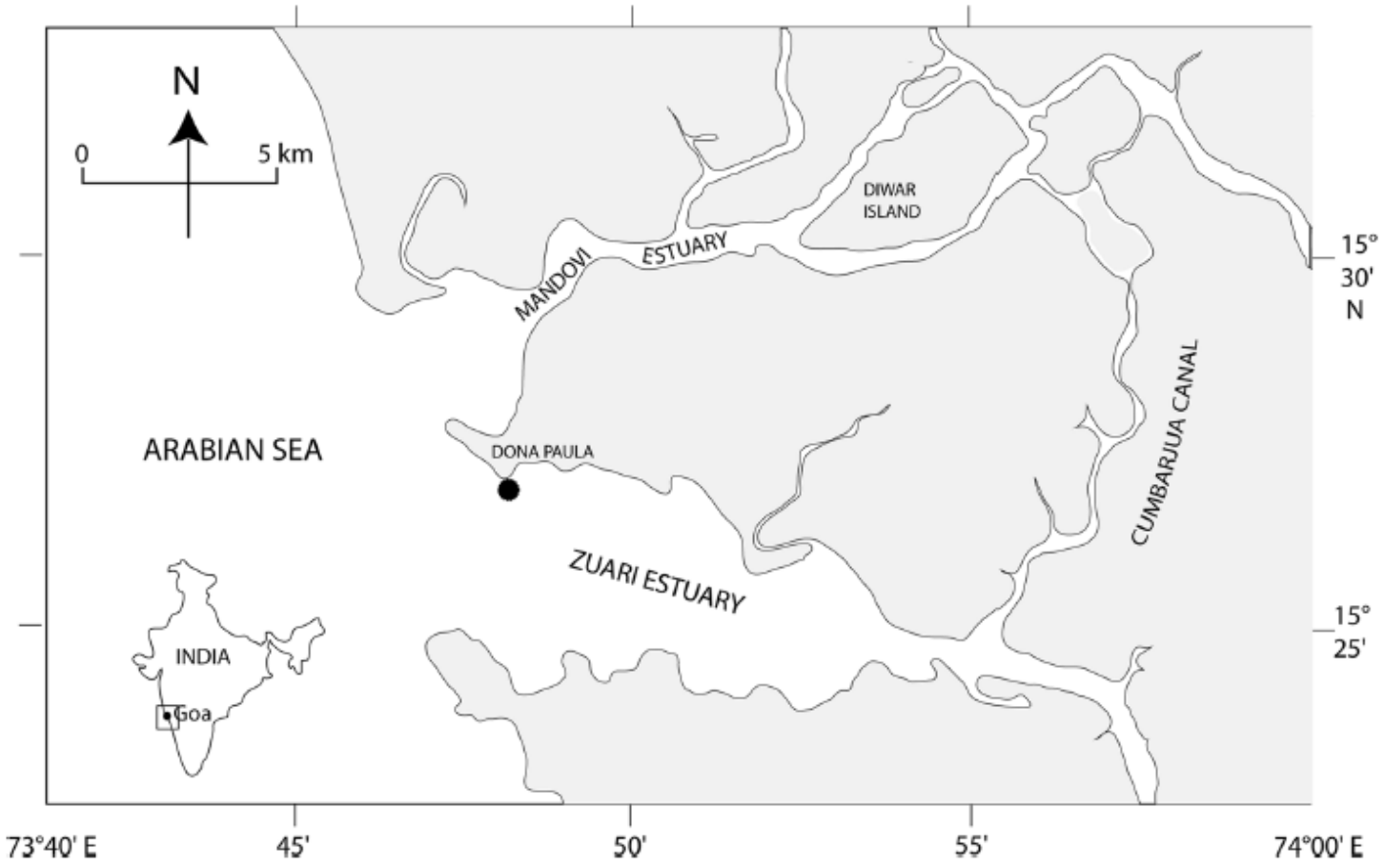

Figure 1

Location of the study area

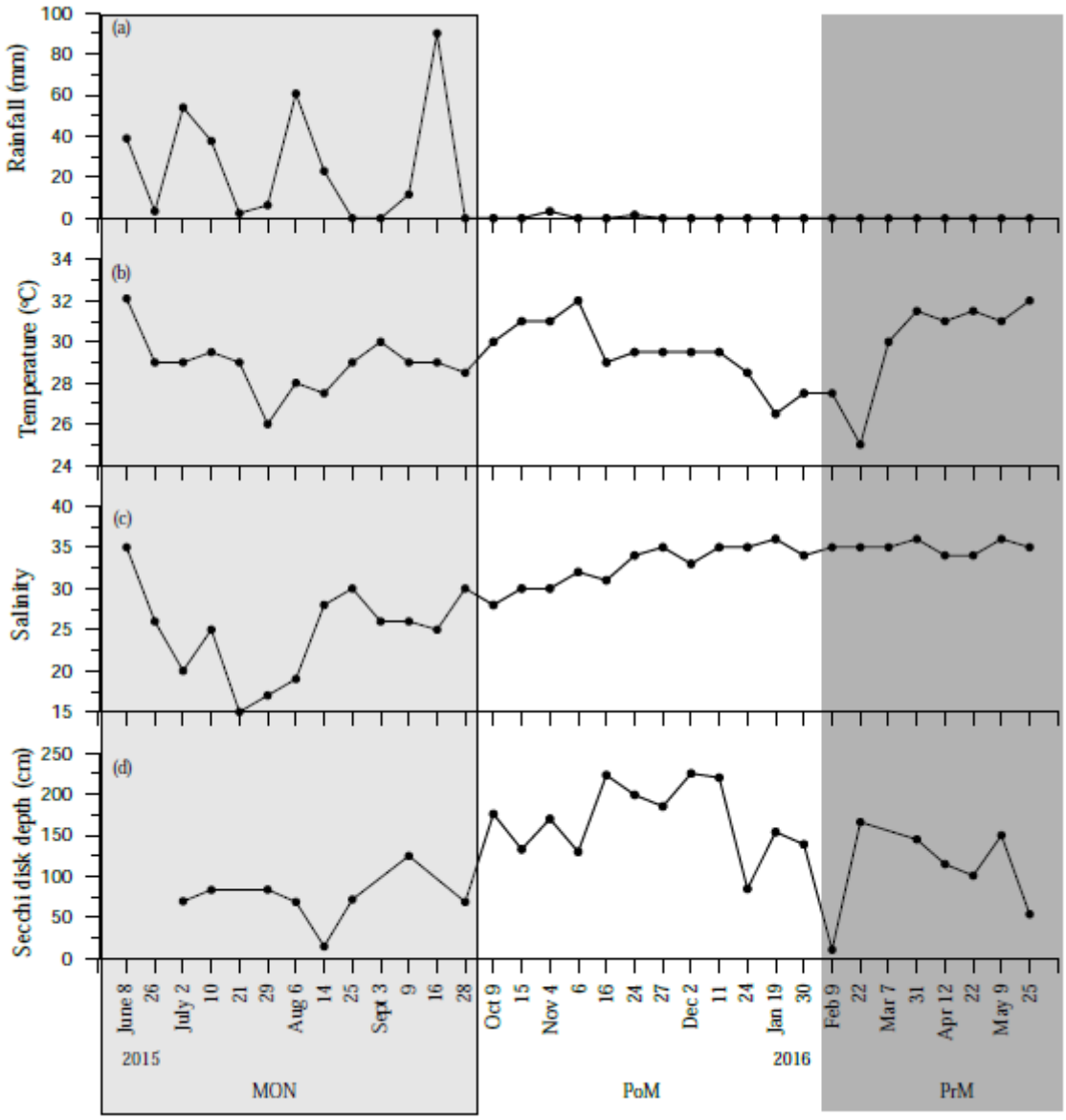

Figure 2

Distribution of environmental parameters at the Dona Paula Bay during the study period (a) rainfall, (b) water temperature, (c) salinity, and (d) Secchi disk depth

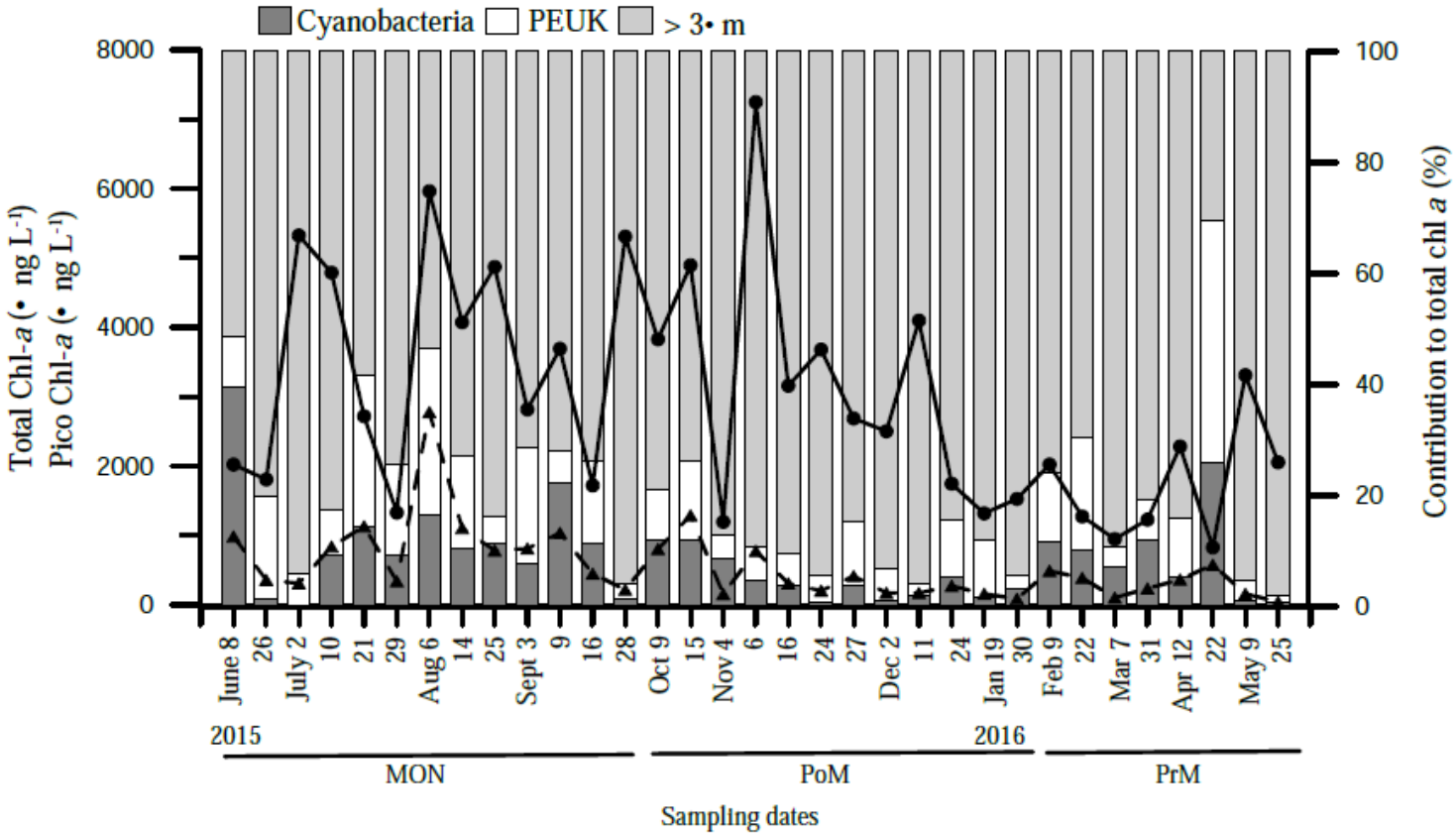

Figure 3

Concentrations of total chl-a, Pico fraction chl-a and relative contribution of Pico to total chl-a biomass

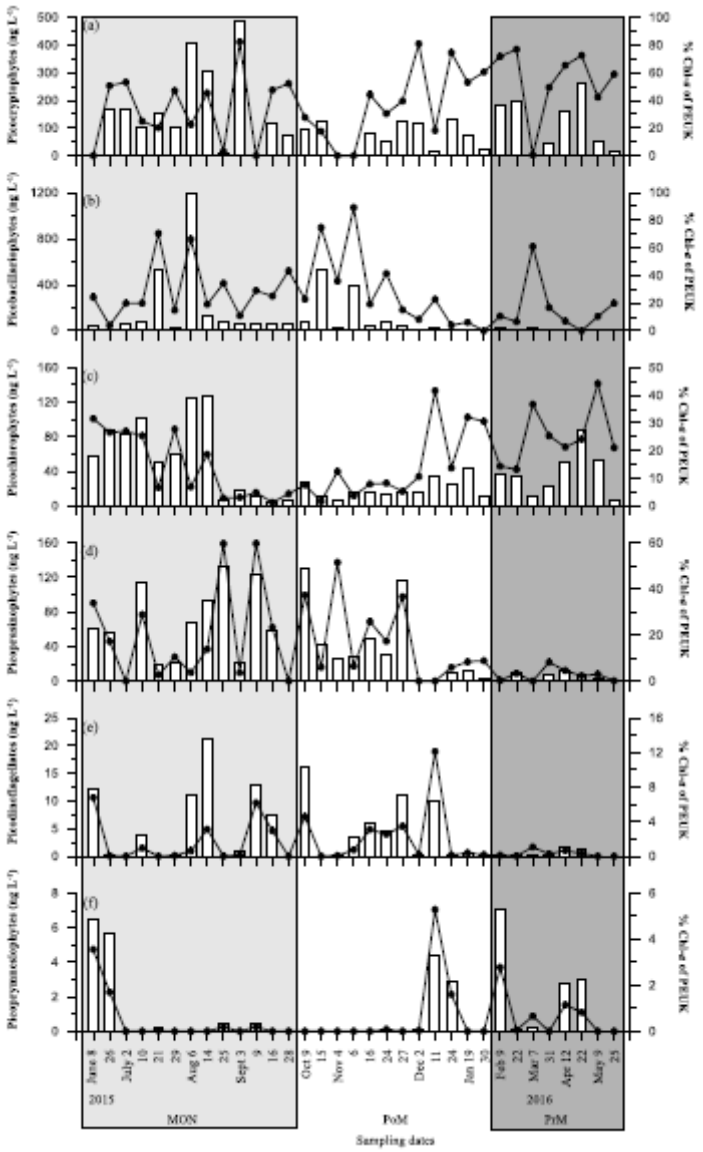

Figure 4

Chl-a biomass concentration of PEUK groups (bar graph) and their individual contribution (%; line graph) to the total PEUK biomass (a) Picocryptophytes, (b) Picobacillariophytes, (c) Picochlorophytes, (d) Picoprasinophytes, (e) Picodinoflagellates and (f) Picoprymnesiophytes

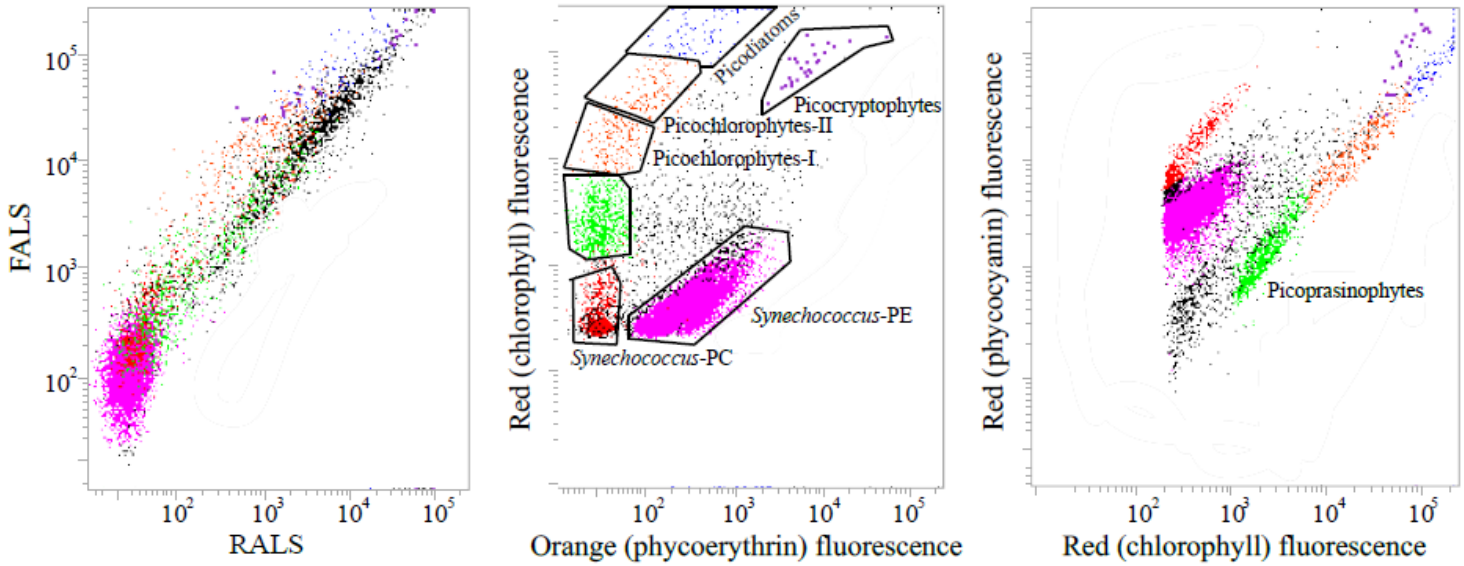

Figure 5

Flow cytograms depicting the picophytoplankton groups from flow cytometric analyses. FALS: Forward Angle Light Scatter; RALS: Right Angle Light Scatter

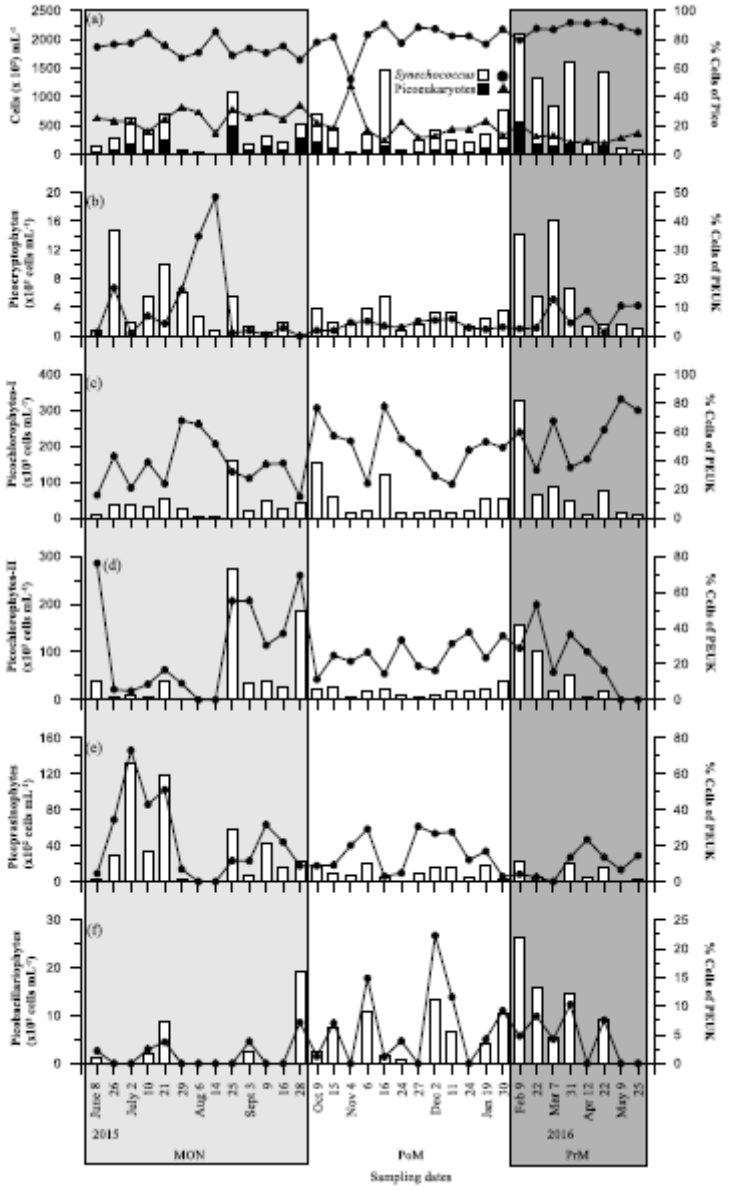

Figure 6

Synechococcus and PEUK cell abundance (bar graph) and contribution to total picophytoplankton (a), PEUK group abundance and their individual contribution (%; line graph) to the total PEUK abundance: Picocryptophytes (b), Picochlorophytes-I (c), Picochlorophytes-II (d), Picoprasinophytes (e), and Picobacillariophytes (f)

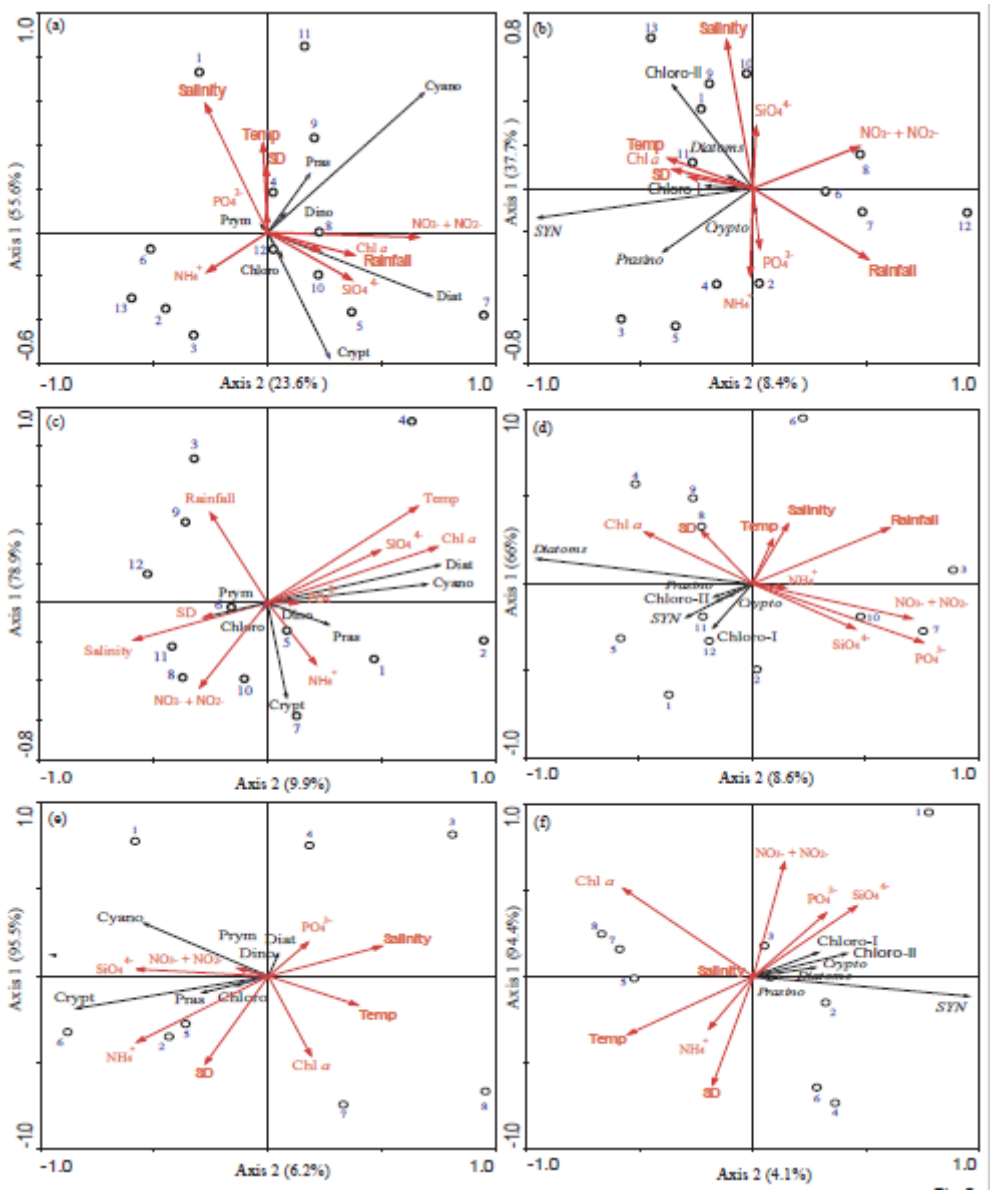

Figure 7

Redundancy Analysis (RDA) between the environmental variables (rainfall, temperature, salinity, SD depth, total chl-a, DIN (NO3-+ NO2-), NH4+, PO43-and SiO44-) and Pico group biomass (a, c, e) and abundance (b, d, f) for the monsoon, post-monsoon and pre-monsoon seasons, respectively

Supplementary Files

This is a list of supplementary files associated with this preprint. Click to download.

- Tables13.docx